POLITECNICO DI TORINO
Repository ISTITUZIONALE

DIGITAL REPLICAS OF BRITISH MUSEUM ARTEFACTS

Original
DIGITAL REPLICAS OF BRITISH MUSEUM ARTEFACTS / Patrucco, G., Bambridge, P., Giulio Tonolo, F., Markey, J., Spano, A.. - In: INTERNATIONAL ARCHIVES OF THE PHOTOGRAMMETRY, REMOTE SENSING AND SPATIAL INFORMATION SCIENCES. - ISSN 2194-9034. - ELETTRONICO. - XLVIII-M-2-2023:(2023), pp. 1173-1180. [10.5194/isprs-archives-XLVIII-M-2-2023-1173-2023]

Availability:
This version is available at: 11583/2980002 since: 2023-07-06T14:33:23Z

Publisher:
Copernicus

Published
DOI:10.5194/isprs-archives-XLVIII-M-2-2023-1173-2023

Terms of use:

This article is made available under terms and conditions as specified in the corresponding bibliographic description in the repository

Publisher copyright

(Article begins on next page)

27 November 2026

The International Archives of the Photogrammetry, Remote Sensing and Spatial Information Sciences, Volume XLVIII-M-2-2023
29th CIPA Symposium "Documenting, Understanding, Preserving Cultural Heritage:
Humanities and Digital Technologies for Shaping the Future", 25–30 June 2023, Florence, Italy

DIGITAL REPLICAS OF BRITISH MUSEUM ARTEFACTS

G. Patrucco[1], P. Bambridge[2], F. Giulio Tonolo[1], J. Markey[2], A. Spanò[1] *

[1] LabG4CH - Laboratory of Geomatics for Cultural Heritage. Department of Architecture and Design (DAD) - Politecnico di Torino, Viale Mattioli, 39, 10125 Torino, Italy (fabio.giuliotonolo, giacomo.patrucco, antonia.spano)@polito.it
[2] FARO Technologies UK Ltd, Great Central Way, Rugby CV21 3XH, United Kingdom (peter.bambridge, jamie.markey)@faro.com

KEY WORDS: digital replicas, close-range photogrammetry, CMM arm scanner, semi-automated processing, geometric and radiometric accuracy, 3D modelling

ABSTRACT:

The digitisation of museum exhibits has played an essential role in geomatics research for generating digital replicas, as it offers the chance to address rather challenging issues. The use of different sensors, ranging from active to passive, and also structured light scanners or hybrid solutions, the various destinations and purposes of the final results combined with the extreme variety of possible objects have made it a field of investigation highly inquired in the literature.
The present study aims to analyse and discuss a digitalisation workflow applied to four Sumerian civilisation masterpieces preserved in the British Museum. The dense and accurate 3D point clouds derived from a specimen of Articulated Arm Coordinate Measuring Machines in collaboration with Faro technologies have twofold roles: ground truth and geometric reference of the final digital replicas. Digital photogrammetry is employed to enrich the models with the relevant radiometric component. The significant contribution results, exploiting co-registration strategies, offer careful guidance of a photogrammetric protocol created in a highly controlled environment combined with skilful expedients and devices. The proposed approach enables the acquisition of high-quality and radiometrically balanced images and improves the possibility of automating the masking procedure before the photogrammetric processing.

1. INTRODUCTION AND FRAMEWORK

The digitisation of small objects has been playing a significant role in the studies characterising the methods and solutions for 3D surveying and modelling cultural heritage (CH) assets. Considering museum collections involving an extraordinary variety of works of art and archaeological finds, a wide range of research experiences have been carried out to identify appropriate solutions due to the thrust provided by the heritage preservation needs promoted by research institutions and programs (Data accessibility and digital preservation, Horizon2020 framework[1]) and by the development of strategies and guidelines aimed to secure the availability and accessibility of museum collections information (ICOM 2017).
The adequate and feasible responses to this critical digitisation request are undoubtedly dependent on the diversified purposes and often not aimed at specific objectives but, at the same time, destined for multiple uses and purposes.
In general, the fine-tuning of image and range-based methods are aimed at obtaining very high geometric and radiometric resolutions to support specialised studies (Francolini et al. 2020), for diagnostic purposes and evaluation of the state of conservation (Donadio et al. 2018), for restoration operations (Girelli et al. 2019), to obtain parametric datasets (Patrucco et al. 2019) or 3D printing (Balletti et al. 2017).
In the context of studies aimed at developing geomatics technologies, significant emphasis has been given to low-cost solutions, often based on structured light scanners (Kersten et al. 2017), and integrated solutions for arranging the massively detailed digitisation of museum-preserved objects (Ritz et al. 2017). Easy-to-use paradigms, rapid acquisition phases and semi-automated processes (Apollonio et al. 2021) are often purposed to support and facilitate the widespread generation of 3D digital replicas. Nowadays, many museums are planning interactive exhibitions to improve and enhance the visitors' experience through interactive museum experiences based on virtual reconstruction technologies (Kersten et al. 2018). At the same time, digital inventories are a crucial present perspective, as witnessed by the experience presented in this paper that focuses on the digitisation of 4 exhibits of the British Museum (BM) selected for a dissemination project.

1.1 The motivation of the research

The digitisation procedures indeed have been planned to aim to obtain high-quality digital replicas suitable for multiple and different purposes: to be able to support further specialised studies, to respond to the needs of the museum institutions and the related need to disseminate the results (generally through open on-line repositories), and to support multimedia projects disclosure.
The ancient works of art selected for this project are masterpieces of the Sumerian civilisation that are kept at the British Museum in London. One of the first goals was to carry out a multimedia video explaining the values of these exhibits to the public of the Iraq Museum in Baghdad.
This first finalisation did not exclude making the replicas so that they can also be used for purposes other than dissemination; the further investigations that are intended to be applied to the models have directed the choice to aim for the maximum geometric and radiometric quality available from market devices.
The materials that make up the four museum artefacts involved in the project (Standard of Ur, Ram in a Thicket, Helmet of Meskalamdug, Gold dagger with scabbard, all of the dimensions of a few dozen of cm) are precious and challenging for digitisation purposes (e.g., shell, red limestone, lapis lazuli, gold,

* Corresponding author

[1] 2030 Digital Compass: the European way for the Digital Decade, Communication from the Commission to the European Parliament, the Council, the European economic and social Committee and the Committee of the Regions, Brussels, 9.3.2021.

copper-alloy, limestone, wood, etc.). Reflective material presents critical issues and, additionally, some elements of the analysed assets, such as the gold leaf representing the typical hairstyle of the Early Dynastic kings of the Helmet, require an extraordinarily high resolution and precision for details modelling.

1.2 Related works

As mentioned, the digitisation of museum artefacts, or in general small works of art, has been highly supported by using different technologies and sensors, ranging from active to passive, and also by structured light scanners or hybrid solutions. The 3D reconstruction applied through the photogrammetric survey based on pipeline Structure from Motion (SfM) and Image matching (IM) is highly appreciated from the cost perspective, which is undoubtedly a significant need in cultural heritage. On the other hand, to make the entire process truly sustainable, both in the acquisition and processing phases, it is necessary to follow precise control procedures for each step (Farella et al. 2022).
Since the use of rotating platforms is almost a forced adoption, it is interesting to consider the study of (Guidi et al. 2020), which examines the lateral displacement of cameras in typical convergent shooting to assess the influence on the final quality of models. Given the well-known consideration that the ratio between the shooting distance and the baseline of images is much larger in the process supported by SfM compared to traditional photogrammetry, they assessed that values comprised about 5 to 6 minimise the RMS errors.
A critical issue that is addressed in a particularly recurrent way is linked to the reflective surfaces of the objects.
(Chen et al. 2007) analysed the emission of light rays in disordered waves from light sources such as LED, light bulbs, and natural light, and affirmed the usefulness of polarising filters applied to the projectors and the camera.
Depending on the reflectivity materials and richness of details requested in the 3D reconstruction, cross-polarised light conditions are strongly suggested, using combined filters for led lighting systems and flashes and controlling the polarisation direction (Hallot & Gil, 2019).
The same authors assess the practical use of colour chart calibration to avoid random colour variations, especially when it is essential to maintain the reliability of the radiometric values of the models. Keeping the same acquiring configuration, exposure, and aperture, the contrast of images increases with the use of polarised light.
Another critical point, which our experience has also made use of, is the attention that must be paid in the acquisition phase to guarantee the chance of supporting the image masking in a semi-automatic form to speed up and optimise the bundle adjustment process.
Considering that the overexposure of the white background enhancing the contrast between objects and the background is undoubtedly an available solution (Vuković et al. 2022), it is also known that such an issue is a crucial concept in Computer Vision, and automated AI methods progressively replace traditional ones (Farella et al. 2022; Patrucco & Setragno 2021).
The CMM technology is used in several industries, including manufacturing, automotive, medical applications, reverse engineering and rapid prototyping, and specific fields requiring certified sub-millimetric accuracy and resolution (Salameh et al. 2023), including CH (Spangher et al. 2017).
A proposal that could be in line with the necessary sustainability to be imprinted on projects involving cultural heritage is the one formulated by (Rodríguez-Martín & Rodríguez-Gonzálvez 2020), which exploits the extreme accuracy of CMM machines to measure GCP to build a calibrated platform for a continuous use foreseen in multiple photogrammetric surveys.

2. METHODOLOGY

2.1 Selected methods: opportunities and constraints

The materials, such as shell, red limestone, lapis lazuli, gold, copper-alloy, limestone, and wood, that make up the four museum artefacts involved in the project are precious and challenging for digitisation purposes. Reflective material presents critical issues, and, additionally, some elements of the analysed assets (e.g. the gold leaf representing the typical hairstyle of the Early Dynastic kings of the Helmet) require an extraordinarily high resolution and precision for details modelling. These aspects have been carefully evaluated for the methodological choice of the digitisation strategy. The selected solution uses a very high-definition scanner for the geometric component and close-range photogrammetry to create metrically controlled textures, enabling high radiometric and geometric precisions.
Essentially, the expected accuracies had to be sub millimetres, and the density of the points envisaged had to allow the representation of millimetre size details or less.
Another constraint to be considered in planning the acquisition phase was the room where the scanning phase took place: a naturally lit storage room with no possibility of darkening the windows. Obviously, the sensing technologies had to foresee not only no contact with the objects but also their limited manoeuvrability by the BM personnel.

2.2 CMM technology applied to museum objects

The geometric complexity of the objects, such as the delicate parts of the bush on which the ram rests, as well as its plumage, the need to scan the internal and external surfaces of the helmet, and the outstanding workmanship of the gold dagger, have recommended the use of the so-called non-contact coordinate measuring machines (CMM) also called AACMM (Articulated Arm Coordinate Measuring Machines).
During the acquisition of the artefacts, the FARO Quantum Max S Model 2.0m Arm with FARO xP Laser Line (LLP) was employed. The used laser scanner was equipped on a 7-Axis FaroArm (https://www.faro.com) (Figure 1). By attaching the laser line probe directly to the articulated arm, 3D data can be fully captured without contact with an object. Measurement points are captured by projecting a beam onto the object's surface, and a camera then "looks" at the beam to determine its location. The laser line probe is fully encoded to the arm, allowing for uninterrupted data transfer. Combined with the FARO 8-Axis Max rotary worktable, the need to relocate or reposition the device or object is virtually eliminated, and the scans can be collected, optimising the time required from the acquisition.
The main specifications of the scan arm are shown in Table 1.

Accuracy	± 15 µm
Repeatability	15 µm 2σ
Stand-off	105 mm
Depth of field	110 mm
Effective scan field	Near field 80 mm Midfield 110 mm Far field 150 mm
Minimum points spacing	20 µm
Maximum points per line	4000 points
Maximum scan rate	600 Hz
Point acquisition rate	Up to 1.2 million points per second
Laser	450 nm/635 nm, class 2

Table 1. Faro Blu xP Laser Line Probe specification and accuracy

The system accuracy for the utilised system is 0.038 mm for Non-Contact Measurement (ScanArm and ScanArm + 8-Axis): based on ISO 10360-8 Annex D.
The FARO Laser Line Probe models produce a visible laser beam, featured by CDRH Class II and IEC Class 2 power level, which is classified as safe and received the authorisation from the British Museum to be used to scan the precious exhibits.
When setting up the on-site system, it is possible to run through the onsite verification process to confirm the system was within the certified and calibrated figure, first by running through a hole compensation procedure with the 6 mm hard probe and then verifying the LLP to the position of the hard probe, by probing a white calibration plate and then scanning the same plate with the LLP. The hard probe was within the required 0.0144 mm, and the Laser Line Probe was within the required 0.0263 mm.
Despite the high productivity guaranteed by the initial calibration, since the Laser Line Probe (LLP) can continue to work continuously after the first inspection, the complete scans of the 4 BM finds required at least 16 hours of work. The generation of the complete, extremely dense clouds requires the use of clustering algorithms for cloud optimisation, able to allow topologically correct meshes without discontinuity errors or duplication of triangles.

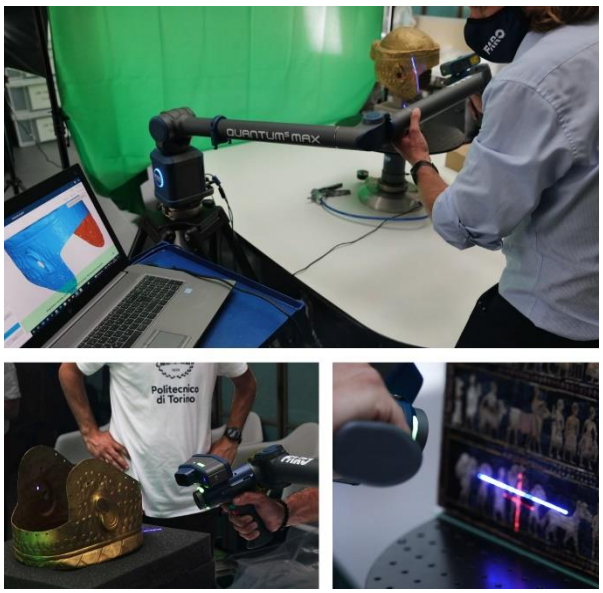

Figure 1. Acquisition of the artefacts using the FARO Articulated Arm Coordinate Measuring Machine.

2.3 Very close-range photogrammetric survey

The photogrammetric 3D survey of the museum artefacts has been designed to address specific issues during the acquisition and processing phases to meet the 3D requirements and boost the semi-automated processing.
Regarding the expected level of detail, it was estimated that according to the artefacts' shapes and sizes, it was necessary to have an average point distance lower than 0.5 mm and, accordingly, a submillimetre precision. To meet this goal, using consolidated formulas (Granshaw 2020), the following survey parameters have been defined:

- Focal length (50 mm);
- Average distance sensor-object (0.5 m - 0.8 m);
- DLSR camera (model: Canon EOS 5DS R) with a sensor size of 24 x 36 mm^2 and image size of 8688 x 5792 pixels;
- Image forward and lateral overlap of at least 80%, using a consolidated close-range photogrammetry convergent acquisition schema for SfM-based approaches. Three different strips have been planned to enable the full coverage of the artefacts with a proper overlap, as shown in Figure 2.

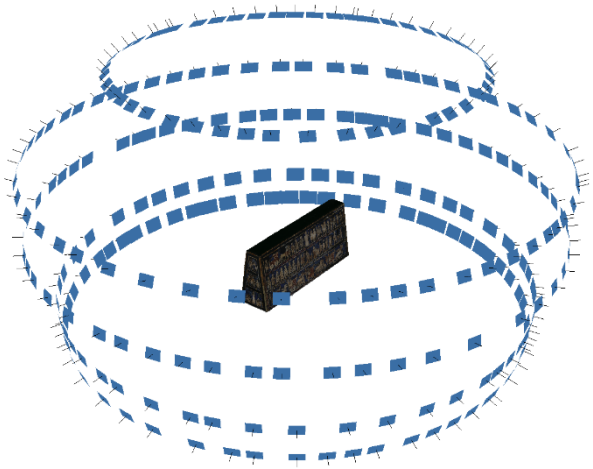

Figure 2. Close-range photogrammetry convergent acquisition schema used for the Standard of Ur artefact.

In Table 1, it is possible to observe the number of acquired images for each dataset. Several hundreds of digital images have been acquired to cover the surfaces of each of surveyed archaeological assets with a sub-millimetre level precision. The average acquisition distance and the average achieved GSD (Ground Sample Distance) are reported.

	N. images	Average acquisition distance (m)	Average GSD (mm)
Standard	288	0.8	0.06
Ram	455	0.5	0.04
Helmet	496	0.6	0.05
Dagger	315	0.7	0.05
Scabbard	276	0.7	0.05

Table 2. Parameters featuring photogrammetric point clouds.

Considering that the museum artefacts could be moved only by museum experts with the required expertise and that the contact with the artefacts needed to be limited, the objects were placed on a motorised rotating platform to optimise the acquisition phase operations described above, i.e. moving the object rather than the camera. The platform movements were controlled by remote control to ensure a regular forward overlap of the convergent images. Images were taken from different tripod heights and acquisition angles to acquire the planned strips with the required lateral overlap,
One of the main concerns related to the image acquisition was associated with the consistency of the illumination on the acquired images, with a twofold goal: i) to minimise the presence of shadows (that negatively impacts the image autocorrelation step) and ii) to avoid reflections due to the artefacts decorations materials.
Therefore, to ensure consistent and homogeneous illumination, two LED panels (by LUPO) equipped with diffusers and four additional flashes mounted on a ring around the camera lens have been used. Additionally, the four flashes have been covered with a polarised filter: the same filter was installed on the camera lens to minimise light reflections fine-tuning the polarised filter orientation (Hallot & Gil 2019).
A remote-release device was used to avoid blurred or smoothed-out images, with an appropriate set of ISO, lens aperture and acquisition time settings.

Finally, a green screen was used to facilitate the automatic selection of the background (using a semi-automatic RGB-based selection procedure) during the masking procedures carried out before the photogrammetric processing (Farella et al. 2022).
The overall set-up of the close-range photogrammetric survey is shown in Figure 3.



Figure 3. 3D close-range photogrammetric survey general set-up, including green screen, artificial LED lights, DSLR camera mounted on a tripod, four flashes mounted on the camera lens ring, and rotating platform.

The image acquisition phase of each artefact started with a preliminary acquisition of a radiometric calibration panel (Calibrite ColorChecker Classic – https://calibrite.com) (Figure 4), repeated for each different configuration of tripod height and viewing angle to enable the radiometric calibration of every single image and a consequent consistency of the radiometry of the final products (Molada-Tebar et al. 2019).



Figure 4. Preliminary acquisition of a radiometric calibration panel for each different acquisition configuration.

Several calibrated scale bars have been positioned on the rotating platform to properly scale the models and validate the results, as shown in Figure 5. An off-the-shelves product has been used – Palaeo3D scale bars (http://palaeo3d.de) – including both linear and orthogonal shaped scale bars, leading to a declared average error of less than 1% of the scale bar length (i.e. less than 0.1 mm when using 0.1 bars scales), and meeting the survey 3D precision requirements. Pre-defined markers printed on each scale bar enable automatic identification in different photogrammetric software platforms, boosting the post-processing workflow's automation level.

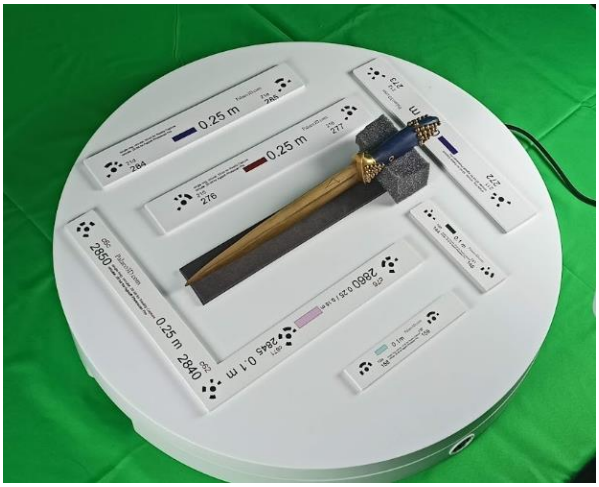

Figure 5. Scale bars and museum artefact positioning on the rotating platform

3. PROCESSING AND QUALITY EVALUATION

The LiDAR and photogrammetric point clouds were aligned through ICP algorithms, enriching the final models with metrically controlled high-resolution radiometric information.

3.1 LiDAR processing and results

FARO RevEng software was used to align the point clouds. Before scanning the artefacts with the LLP, the Automatic Exposure algorithm was selected in the LLP settings. The Automatic Exposure mode analyses the material during scanning and automatically adjusts the Exposure and Laser Intensity during data collection.
The top surface of the 8-Axis scanning platform was scanned, and a clipping plane was generated before the artefacts were placed on the platform. The clipping plane is activated and automatically removes points captured on the top surface.
The typical workflow followed:

- Capture Scans - Collected raw point data was selected, keeping 100% of the points captured with no enhancements to the scanned data.
- Clean up Scans - FARO RevEng software automatically selects erroneous data points that fall outside of the artefacts' main cluster of points. These outliers are reviewed before removal.
- Point Cloud Registration consists in aligning one or more point clouds. Typically, the registration process is split into the following phases:
    1. First Guess: the first guess is the first phase of the point cloud alignment. A rough manually assisted transformation is performed – i.e. picking common points on both point clouds – in order to enable the subsequent registration procedures.
    2. Point Cloud Sampling: Determination of a subset of points to use in the Iterative Closest Point (ICP) process.
    3. ICP registration: Based on the subset sample defined in the previous step, an ICP registration with the aim of calculating a better transformation in each iteration until the convergence rule is verified.
    4. Calculate alignment accuracy: The alignment accuracy is calculated at the end with the resulting transformation.

The discrepancies observed between adjacent scans after the ICP optimisation steps are of a sub-millimetric order of magnitude. To provide an example, regarding the global registration of the two scans of the helmet, the residual surface error was 0.021 mm.

3.2 Photogrammetric processing and results

As far as the photogrammetric approach adopted in the presented research, the acquired digital images have been processed according to the following steps:

- Step 1: Radiometric calibration of the images.

Before proceeding with photogrammetric processing, the images were radiometrically calibrated using the radiometric calibration panel (acquired at the beginning of each acquisition). The acquired datasets have been processed according to the following workflow:

- Pre-processing of the images – specifically acquired for the calibration procedure – using Adobe Camera Raw software. A white balance adjustment procedure has been carried out exploiting the white frame of the calibration panel.
- The raw images have been imported into the ColoreChekcer Camera Calibration platform, where a radiometric calibration has been performed using the calibration panel as a reference. A digital colour profile (.dcp) has been generated and exported.
- Calibration and colour transforming of the entire photogrammetric block using the exported colour profile in Adobe Camera Raw plug-in. During the process, the edges of the raw images belonging to the acquired datasets edges have been enhanced. Subsequently, the datasets have been exported in .jpg file format in order to be used for the photogrammetric process (Figure 6).

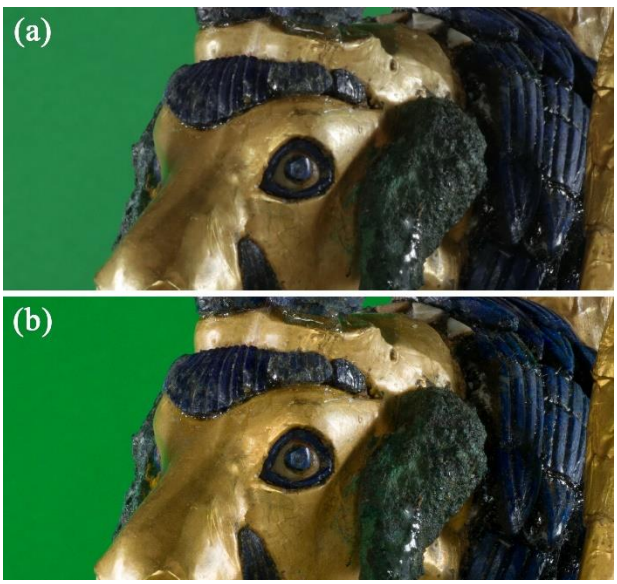

Figure 6. (a) Acquired digital image; (b) Digital image after the radiometric calibration procedure.

- Step 2: Semi-automatic generation of the exclusion masks.

A semi-automatic approach for generating the exclusions masks have been applied in the presented case. Usually, using the rotating platform strategy described in the previous sections – allowing a significant enhancement in efficiency during the acquisition of the images – using exclusion masks is almost mandatory since the background is stationary while the acquired object is moving. This could cause errors during image orientation and compromise the 3D reconstruction results (Patrucco & Setragno 2021). In this case – exploiting the green screen set up in the background – a batch process was run on all images to perform an RGB-based selection of the green pixels and generate .png binary masks.

- Step 3: Metric validation of the scale bars.

To evaluate the accuracy of the metric bars positioned on the acquisition stage to be used as reference for scaling the reconstructed 3D models, a test has been carried out using a calibrated Invar metric bar (length: 1000.165 mm) (Figure 7). Five of the used scale bars have been positioned next to the Invar metric bar. Subsequently, a photogrammetric acquisition has been carried out using the same DSLR camera used to acquire the artefacts (model: Canon EOS 5DS R) from a similar distance (approximately 0.6 m), leading to a roughly identical GSD. 31 images have been acquired. The images have a high overlap (>80%), following the photogrammetric criteria described in the previous sections. The images have been oriented, and the achieved 3D model has been scaled using the scale bars as a reference, while the Invar metric bar has been used to evaluate the accuracy (Figure 8). The RMSE observed on the scale bars is approximately 0.001 m, while the RMSE observed on the Invar metric bar used as check scale bar is submillimeter-level (ca. 0.0003 m), confirming the high accuracy of the used calibrated scale bars.



Figure 7. Calibrated Invar metric bar.

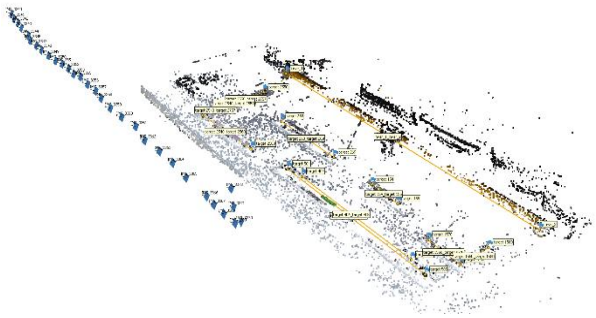

Figure 8. Oriented images, sparse cloud of tie points and scale bars.

- Step 4: SfM-based 3D photogrammetric reconstruction.

The acquired datasets have been processed using the SfM-based software Agisoft Metashape (build 1.8) following a standard workflow consisting of i) interior orientation of the camera using a self-calibration approach; ii) relative orientation of the images and generation of a sparse cloud of tie points; iii) scaling the 3D model using the scale bars (in this case the efficiency of this step has been greatly enhanced by the possibility of automatically detecting and identifying the pre-defined markers, avoiding a manual and time-spending procedure); iv) generation of a dense coloured point cloud; v) generation of a 3D mesh; vi) generation of a high-resolution UV map. Approximately one-third of the scale bars were used to assess the metric accuracy of the models. Regarding the scale bars used for scaling and the ones used to provide an accuracy check to the generated models, the observed errors are sub-millimetric (coherently with the test carried out using the Invar metric bar). In Figure 9, it is possible to observe the achieved textured 3D models of the acquired artefacts.



Figure 9. Textured 3D models of the acquired archaeological artefacts.

4. COMPARISON BETWEEN THE METHODOLOGIES AND DISCUSSION

The results described in the previous sections have been compared in terms of the level of detail and density, focusing on the spatial resolution and geometric features of the generated point clouds. However, before proceeding with the comparisons, the first consideration concerns the time required to acquire the primary data from which to derive the 3D models. Although neither of the two methods has outperformed the other in terms of achieved results, the laser scanning method required approximately 16 hours to complete the acquisition of the measured assets, while the image-based approach – despite the strategies adopted to optimise the data collection phase, such as the use of the rotating robotic platform – required a higher amount of time (ca. 30 hours). This highlights the need to develop new strategies and workflows to improve the efficiency of these acquisition procedures further.

Instead, concerning the comparison between the different acquired 3D data, the point clouds acquired using the laser scanning methodology are composed of a number of points that are an order of magnitude greater than those generated with the photogrammetric technique. This can be observed in Table 3, where the number of points of each point cloud – collected with the two different methodologies – is reported and compared. Consequently, the point density of the laser scanning data is significantly higher. The average distance detected between points in each LiDAR scan is between 0.02 and 0.05 mm, while that observed on photogrammetric point clouds has a range between 0.06 and 0.17 mm. In Table 4, a significant comparison of the results obtained in terms of information density and quality of the final resolution of the models is reported (densities of the acquired point clouds, measured in points/cm^2, and the average distances between the points).

	Number of points	
	Laser scanning	Photogrammetry
Standard of Ur	ca. 217 million	ca. 16 million
Ram in a Thicket	ca. 176 million	ca. 44 million
Helmet	ca. 263 million	ca. 42 million
Gold dagger	ca. 41 million	ca. 3 million
Scabbard	ca. 23 million	ca. 3 million

Table 3. Number of points characterising LiDAR and photogrammetric clouds.

	Density [points/cm^2]		**Average point distance [mm]**	
	Laser scanning	SfM	Laser scanning	SfM
Standard	> 50,000	> 5,000	ca. 0.04	ca. 0.14
Ram	> 100,000	> 30,000	ca. 0.03	ca. 0.06
Helmet	> 175,000	> 25,000	ca. 0,02	ca. 0.06
Dagger	> 35,000	> 3,500	ca. 0,05	ca. 0,17
Scabbard	> 70,000	> 10,000	ca. 0.04	ca. 0.10

Table 4. Density information characterising LiDAR and photogrammetric clouds.

Regarding the metric assessment of the achieved results, in addition to the tests carried out with the scale bars, cloud-to-cloud comparisons were performed between the point clouds generated using the methodologies described in the previous sections. The laser scanning models (given their nominal precision) have been used as ground truth for the metric validation of the photogrammetric products. The two point clouds have been registered in the same coordinate system using an ICP registration procedure. Subsequently, a discrepancy analysis has been carried out to evaluate the presence of any deviations between the two considered surfaces. The performed analyses have proved the high-quality results of the photogrammetric models, which can be interpreted as characterised by an average relative accuracy of about 0.5 mm. In Figure 10 – as an illustrative example – it is possible to observe the analysis performed on the ram in a Thicket point clouds. In this case, the observed deviations between LiDAR data and photogrammetric data are lower than 0.5 mm for 97.7% of the considered points.

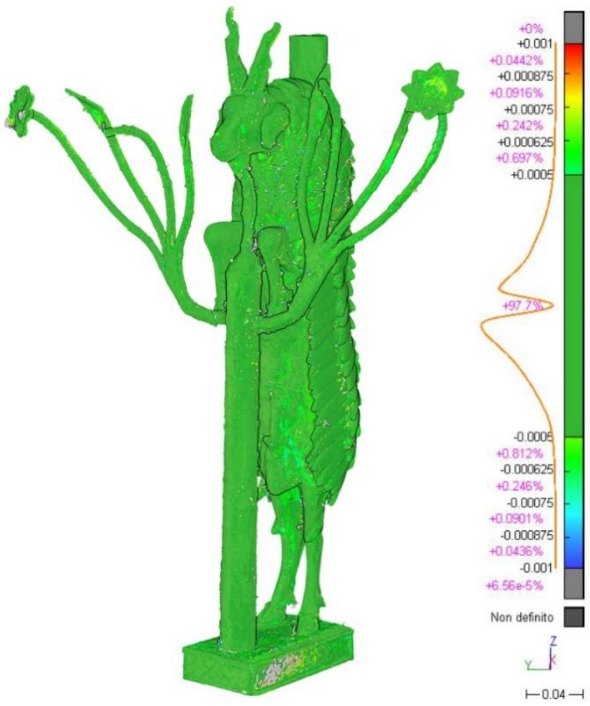

Figure 10. Distance analysis between the photogrammetric and laser scanning point clouds of the ram in a Thicket artefact, highlighting an average discrepancy lower than ± 0.5 mm.

Concerning the geometric features, from a preliminary visual inspection, it is possible to observe that – as expected, considering the higher point density and spatial resolution – the level of detail in the point cloud derived from the laser scanning method is greater than that found in the photogrammetric point cloud (Figure 11). This does not mean that with an image-based

approach, it is not possible to achieve a similar density of information and geometric level of detail. However, to obtain a similar result, it would be necessary to significantly reduce the acquisition distance (in order to obtain a higher GSD). Consequently, the number of acquired images necessary for 3D reconstruction would be much higher, causing an increase in terms of overall file size, file storage, and computational effort required for SfM-based photogrammetric reconstruction.

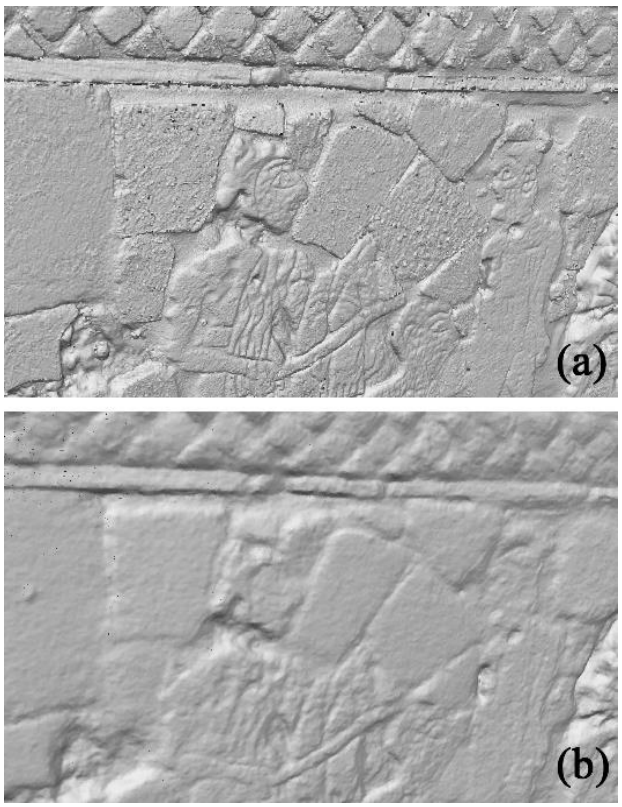

Figure 11. Particular of the Standard of Ur artefact. (a) Point cloud derived from laser scanning survey; (b) Point cloud derived from the image-based approach.

However, one of the advantages of the image-based approach is represented by the possibility of acquiring the radiometry of these objects in order to generate added-value metric products or high-resolution textures (specifically, UV maps for the 3D models). This aspect represents a valuable opportunity, especially in order to document not only the geometry of a museum object but also the materials it is made of. This latter aspect represents a crucial point when considering the conservation and restoration of these artefacts since material consistency represents one of the most essential pieces of information.

Additionally, it is necessary to underline another aspect connected to the replicability of the proposed workflows. While digital photogrammetry represents a relatively economical solution, and it is increasingly widespread in many museum digitisation projects (Guidi et al. 2017; Patrucco et al. 2019), the typology of laser scanner used during this research it is generally used in the metrology field for industrial applications. As far as the field of cultural heritage is concerned, and specifically when the digitisation of movable heritage is involved, these kinds of instruments are not widely employed in the CH field, and they are used only for high-profile digitisation projects (also due to the high costs of these solutions), often thanks to collaborations with companies active in the field of metrology and measurements.

Finally, a concluding remark concerns the opportunity to integrate the two different 3D metric products achieved during the research described in this paper in order to obtain a hybrid 3D model characterised by the spatial resolution of the laser scanning point cloud and the radiometry derived from the high-resolution digital images used for the generation of the photogrammetric model. In fact, exploiting the common reference system of the 3D models derived from the LiDAR approach and the image-based methodology – since the images are oriented in the same reference system and can be projected onto the surface model derived from laser scanning technique – it is possible to colourise the LiDAR point cloud (Figure 12) or generate a high-resolution photogrammetric UV map, to provide a high-resolution texture to the laser scanning model.

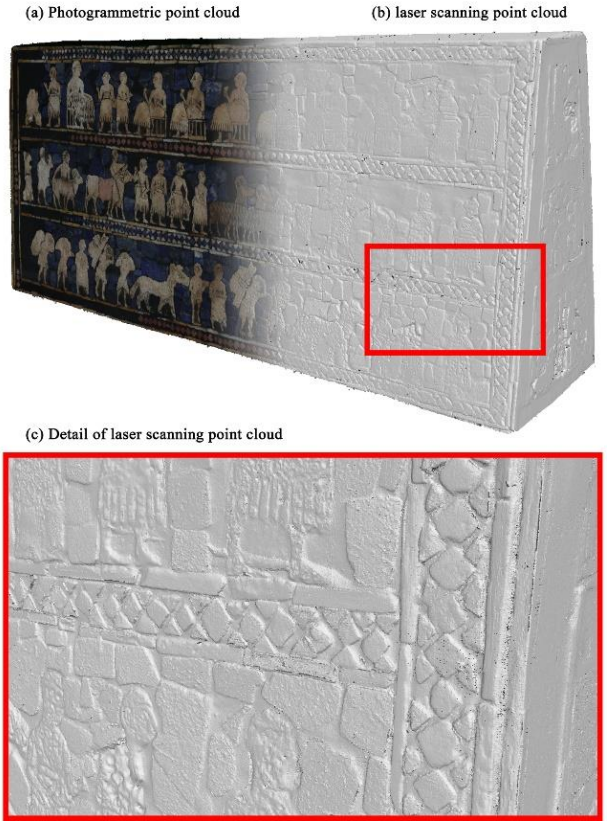

Figure 12. (a) Photogrammetric point cloud (Standard of Ur); (b) Laser scanning point cloud; (c) Detail of laser scanning point cloud.

5. CONCLUSIONS AND FUTURE PERSPECTIVES

As expected, the final dense, accurate, and high-resolution 3D models derived from the integrated methods can perfectly fit more than one goal foreseen at the beginning of the digitisation project, confirming the completeness, timeliness, usability, and versatility of integrated approaches. Controlled point clouds and mesh decimation processes enable adapting the final configuration to different needs ranging from further analyses requiring high-quality geometric and radiometric contents to multimedia navigation of enriched 3D models focusing on disseminating initiatives.

As a future perspective, the authors plan to develop further investigations based on the digital replicas, to enhance the knowledge concerning the restoration works that occurred to the surveyed assets (especially to the standard of Ur, extensively restored in the seventies) and possibly to investigate other aspects related to the artefacts surfaces of the objects, exploiting the exceptional high (geometric and radiometric) resolution of the 3d models.

6. ACKNOWLEDGEMENTS

The authors warmly thank Carlo Lippolis, director of CRAST (Centro Ricerche Archeologiche e Scavi di Torino per il Medio Oriente e l'Asia), for the invitation to participate in the digitisation project; we are also very grateful to the British Museum Middle East Department, especially to Sebastien Rey and Nancy Highcock. The digital replicas are also subject to a dissemination project consisting of a multimedia video for the Iraq Museum in Baghdad (entitled "A Journey to the Sumer Land. Sumerian Masterpieces in the Iraq Museum"). The video illustrates the history of the object's discovery and partly the data acquisition phase. The video will be available as soon as officially presented (hopefully on July 2023) at the following link: https://youtu.be/UaV2HuNKCcw.

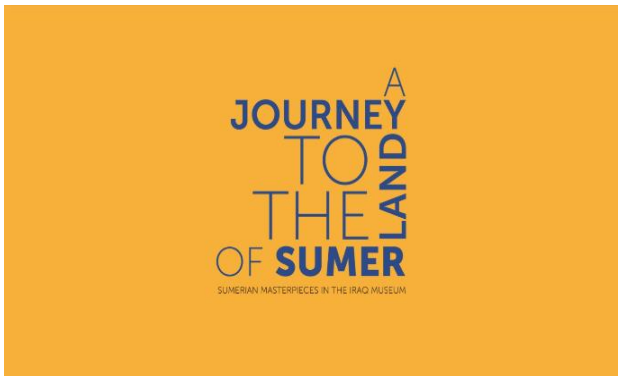

Figure 13. Preview of the opening screen of the video "A Journey to the Sumer Land. Sumerian Masterpieces in the Iraq Museum".

7. REFERENCES

Apollonio, F. I., Fantini, F., Garagnani, S., Gaiani, M. A., 2021. Photogrammetry-Based Workflow for the Accurate 3D Construction and Visualization of Museums Assets. *Remote Sensing*, 13(3), 486.

Balletti, C., Ballarin, M., Guerra, F., 2017. 3D printing: State of the art and future perspectives. *Journal of Cultural Heritage*, 26, 172-182.

Chen, T., Lensch, H. P. A., Fuchs, C., Seidel, H.-P., 2007. Polarisation and Phase-Shifting for 3D Scanning of Translucent Objects. In: *Proceedings of IEEE Computer Society Conference on Computer Vision and Pattern Recognition (CVPR)* Minneapolis, pp. 1-8.

Donadio, E., Spanò, A., Sambuelli, L., Picchi, D., 2018. Three-Dimensional (3D) Modelling and Optimization for Multipurpose Analysis and Representation of Ancient Statues. In: Remondino, F., Georgopoulos, A., Gonzalez-Aguilera, D., Agrafiotis, P., (eds.). Latest Developments in Reality-Based 3D Surveying and Modelling, MDPI, Basel, Switzerland, 95-118.

Farella, E. M., Morelli, L., Rigon, S., Grilli, E., Remondino, F., 2022. Analysing Key Steps of the Photogrammetric Pipeline for Museum Artefacts 3D Digitisation. *Sustainability*, 14(9), 5740.

Francolini C., Girelli, V. A., Bitelli G., 2020. 3D image-based surveying of the safe of the Obellio Firmo Domus in Pompeii. *Int. Arch. Photogramm. Remote Sens. Spatial Inf. Sci.*, XLIII-B2-2020, 1389-1394.

Girelli, V. A., Tini, M. A., Dellapasqua, M., Bitelli, G., 2019. High-resolution 3D acquisition and modelling in Cultural Heritage knowledge and restoration projects: the survey of the Fountain of Neptune in Bologna. *Int. Arch. Photogramm. Remote Sens. Spatial Inf. Sci.*, XLII-2/W11, 573-578.

Guidi, G., Malik, U. S., Frischer, B., Barandoni, C., Paolucci, F, 2017. The Indiana University-Uffizi project metrological challenges and workflow for massive 3D digitization of sculptures. *Proceedings of the 2017 23rd International Conference on Virtual System & Multimedia (VSMM)*, pp. 1-8.

Guidi, G., Shafqat Malik, U., Micoli, L.L., 2020. Optimal Lateral Displacement in Automatic Close-Range Photogrammetry. *Sensors*, 20(21), 6280.

Hallot, P., Gil, M., 2019. Methodology for 3d acquisition of highly reflective Goldsmithing artefacts. *Int. Arch. Photogramm. Remote Sens. Spatial Inf. Sci.*, XLII-2/W17, 129–134.

Granshaw, S. I., 2020. Photogrammetric terminology: fourth edition. *The Photogrammetric Record*, 35(170), 143-288.

Kersten, T. P., Tschirschwitz, F., Deggim, S., 2017. Developement of a virtual museum including a 4D presentation of building history in virtual reality. *Int. Arch. Photogramm. Remote Sens. Spatial Inf. Sci.*, XLII-2/W3, 361–367.

Kersten, T. P., Lindstaedt, M., and Starosta, D., 2018. Comparative Geometrical Accuracy Investigations of Hand-held 3D Scanning System - an Update. *Int. Arch. Photogramm. Remote Sens. Spatial Inf. Sci.*, XLII–2, 487–494.

Molada-Tebar, A., Marqués-Mateu, Á., Lerma, J. L., 2019. Correct use of color for cultural heritage documentation. *Int. Arch. Photogramm. Remote Sens. Spatial Inf. Sci.*, IV-2/W6, 107-113.

Patrucco, G., Rinaudo, F., Spreafico, A., 2019. A new handheld scanner for 3D survey of small artifacts: The Stonex F6. *Int. Arch. Photogramm. Remote Sens. Spatial Inf. Sci.*, XLII-2/W15, 895-901.

Patrucco, G., Setragno, F., 2021. Multiclass semantic segmentation for digitisation of movable heritage using deep learning techniques. *Virtual Archaeology Review*, 12(25), 85-98.

Ritz, M., Knuth, M., Santos, P., Fellner, D. W., 2018. CultArc3D_mini: Fully Automatic Zero-Button 3D Replicator. *GCH 2018: Eurographics Workshop on Graphics and Cultural Heritage*, 1-10.

Rodríguez-Martín, M., Rodríguez-Gonzálvez, P., 2020. Suitability of Automatic Photogrammetric Reconstruction Configurations for Small Archaeological Remains. *Sensors*, 20(10), 2936.

Salameh, R., Yu, P., Yang, Z., Tsai, Y.-C., 2022. Evaluating Crack Identification Performance of 3D Pavement Imaging Systems Using Portable High-Resolution 3D Scanning. *Transportation Research Record*, 2677(1), 529–540.

Spangher, A., Visintini, D., Tucci, G., Bonora, V., 2017. Geomatic 3D modeling of a statue (also) for structural analysis and risk evaluation: The example of San Giovannino Martelli in Florence. *Int. Arch. Photogramm. Remote Sens. Spatial Inf. Sci.*, XLII-5/W1, 61–68.

Vuković, M., Balen, J., Potrebica, H., Mađerić, M., Španiček, V., 2022. 3D digitization of museum artefacts within the interreg iron age Danube project. *Int. Arch. Photogramm. Remote Sens. Spatial Inf. Sci.*, XLIII-B2-2022, 1159-1165.